



Tracking Fatigue Crack Growth of Aluminum Alloy (1050A) under Vibratory Stresses

Prof. Dr. Abdullah Dhayea Assi¹ , Dr. Haider Hussein Hamad²

Abstract

Fatigue cracks have been traced in 1050A aluminum alloy; All the studies and research that have been examined study cracks as short and long cracks, that is, two phases, but through the study it became clear that cracks grow and progress in three phases, the first phase through the microscopic granule, the second phase through the granule to the extent of approximately one millimeter, and the third and final phase to the point of fracture. by phase The first is through the grain size and is called (microscopic short cracks MSC), the second stage is across the grain up to one millimeter is called (the physical short cracks PSC) and the third stage is to the extent of the fracture is called (the long cracks LC). The case of different vibration stresses and factors affecting crack growth in each phase was also studied, and a mathematical model was built that consisted of three equations, each equation representing the cracks' behavior in each phase. The proposed model was also evaluated and compared with a previous proposed model for the same material with practical results. More safety compared to the practical results and the previous model, and this is what is required in the parts from which aircraft fuel tanks are made, as well as in the manufacture of pipelines that carry fuel inside aircraft and for the designer to be in a state of safety when designing aircraft parts. Two MATLAB programs are designed to perform calculations to collect results. The first program to calculate the practical constants and the second to make the calculations required to complete the work schedules.

Keywords: Fatigue, Crack Growth, (1050A) Aluminum Alloy, vibration stresses

تتبع نمو شقوق الكلال لسبيكة الألمنيوم (1050A) تحت الاجهادات الاهتزازية المختلفة
أ.د. عبدالله ضايح عاصي¹ ، م.د. حيدر حسين حمد²

المستخلص

تم تتبع شقوق الكلال في سبيكة الألمنيوم 1050A ؛ وكل الدراسات والبحوث التي تم الاطلاع عليها تدرس الشقوق على انها شقوق قصيرة وطويلة اي بطورين ولكن من خلال الدراسة اتضح ان الشقوق تنمو وتتقدم بثلاث اطوار ، الطور الاول خلال الحبيبية المجهرية ، والطور الثاني عبر الحبيبية الى حد ملمتر واحد تقريبا ، والطور الثالث والاحير لحد الكسر وكما يلي :

- 1- الطور الاول خلال حجم الحبيبية وتسمى (الشقوق القصيرة المجهرية MSC)
- 2- الطور الثاني عبر الحبيبية الى حد ملمتر واحد وتسمى (الشقوق القصير الفيزيائية PSC)
- 3- الطور الثالث لحد الكسر وتسمى (الشقوق الطويلة LC)

تم كذلك دراسة حالة الاجهاد والعوامل المؤثرة على نمو الشق بكل طور وبناء نموذج رياضي يتألف من ثلاث معادلات كل معادلة تمثل تصرف الشقوق في كل طور وكذلك تم تقييم النموذج المقترح وبمقارنته مع نموذج سابق مقترح لنفس المادة مع النتائج العملية اتضح ان النموذج المقترح يعطي حالة امان اكثر مقارنة مع النتائج العملية والنموذج السابق وهذا ما مطلوب في الاجزاء التي تصنع منها خزانات الوقود للطائرات وكذلك في صناعة شبكات الانابيب الناقلة للوقود داخل الطائرات ولكي يكون المصمم في حالة امان عند تصميمه لاجزاء الطائرة.

Affiliation of Authors

¹ Department of Mechanical Engineering, College of Engineering, University of Baghdad, Iraq, Baghdad, 10001

² Department of Petroleum Engineering, College of Engineering, University of Baghdad, Iraq, Baghdad, 10001

¹drabdullahdhayea@uobaghdad.edu.iq

²Haider.hussein@coeng.uobaghdad.edu.iq

¹ Corresponding Author

Paper Info.

Published: June 2024

انتساب الباحثين

¹ قسم الهندسة الميكانيكية، كلية الهندسة، جامعة بغداد، العراق، بغداد، 10001

² قسم هندسة النفط، كلية الهندسة، جامعة بغداد، العراق، بغداد، 10001

¹drabdullahdhayea@uobaghdad.edu.iq

²Haider.hussein@coeng.uobaghdad.edu.iq

¹ المؤلف المراسل

معلومات البحث

تاريخ النشر: حزيران 2024

الكلمات المفتاحية: الكلال، نمو الشقوق، سبيكة الألمنيوم 1050A، الاجهادات

1. Introduction

Failure that occurs under repeated periodic loads is called Fatigue Failure. This type of failure goes through several phases. The first stage is crack initiation, the second stage is crack propagation, and the third stage is complete failure [1,2], and the small cracks of fatigue generally arise at the inclusions or in areas of stress concentration such as sharp edges and slip beams [3], and many researchers, including [4][5][6] have concluded that the fatigue cracks of the aluminum alloy with the symbol (1050A) Coarse slip lines are associated with high stresses, while impurities are associated with lower stresses. Research has shown [6][7] that short cracks grow faster than long cracks and continue to grow rapidly until they reach a strong structural barrier that limits their growth, which represents the transition point from short cracks to long cracks until they overcome this resistance to disability to return and grow at lower rates with constant acceleration. Literature review concerned with studying this phenomenon on the basis that it represents the growth of cracks and their progression until failure occurs without taking into account the behavior of these cracks and he was among the first researchers in this field (Paris) [8,9] where he described the relationship of crack growth and its speed with a factor called stress intensity factor (K) Since this parameter describes the distribution of stresses at the top of the crack, so the stress coefficient in the case of a rapid fracture of the engineering part is called the fracture toughness. As for the critical stress intensity factor (K_c), it depends on the type of metal, the length of the crack, the engineering

stress, temperature and thickness of the engineering part. And he concluded that these cracks increase their speed as they progress in service, and that the relationship he created is represented by the following equation, which is called (Paris Equation):

$$\frac{da}{dN} = C(\Delta K)^m \quad \dots\dots\dots(1)$$

Where:

da/dN = the crack speed (or crack growth rate).

ΔK = The range stress intensity factor

C,m = Constants that depend on the material used and the value of (m) ranges between (2-4) for most materials, including aluminum alloys [10].

In addition to the importance of studying different stresses on the life of fatigue, several studies were conducted that addressed the effect of different stresses, including studies carried out by researchers as follows: The fatigue phenomenon was studied for the aluminum alloy and "Duralumin". The research included conducting tests on samples under fixed and variable amplitude stresses in order to study the effects of stress sequence and accumulated damage [11, 12, 13]. Another researcher conducted a study of the rate of crack growth and the accumulation of fatigue damage for an alloy of low carbon steel under constant and variable amplitude bending stresses and with a constant stress ratio and it was concluded that "the greater the applied stress, the less the number of cycles required for failure, i.e. the shorter the fatigue life" [14,15,16]. The effect of tempering on the fatigue strength of medium

carbon steel (CK 45) was studied, using various heat treatments including water quenching. The stress tests were performed under constant amplitude stresses with a strain ratio ($R = -1$). Two models are proposed to evaluate the fatigue life of quenched and tempered medium carbon steels at different temperatures. The first model was derived from the FCG rate equation (da/dN) while the second model was derived from the stress intensity factor (K) equation [17]. It is clear from Equation No. (1) that this curve has nothing to do with cracks and their behavior, as a certain limit can be extracted from the above equation at which fracture cannot occur, and this limit was called the fatigue limit. For the purpose of extracting this limit, it was agreed that the number of turns should be Equal to (10^7) at this limit [8,18], especially in non-ferrous metals such as aluminum. This means that the age of the sample determines the fatigue limit for ferrous metals, which is infinity, while for non-ferrous metals it reaches (10^8) or more. Therefore, it is preferable to study the behavior and growth of cracks, especially for non-ferrous metals such as aluminum, for the reason that there is no specific fatigue limit under which the age is

infinity Accordingly, attention should be paid to tracking the cracks and knowing when they stop and what is the factor that causes them to grow after they stop [19].

The focus of this research has been on tracing the fatigue cracks of aluminum alloy 1050A because of the wide practical applications of this alloy, especially in the manufacture of fuel tanks for aircraft, as well as in the manufacture of pipe networks carrying fuel inside aircraft, pharmaceutical applications and food containers, due to the features that this alloy possesses from lightness Good weight and resistance to chemical corrosion [20].

2. Experimental work

2.1 The Samples Preparing

The metal used was obtained from the local market in the form of round bars measuring ($2 * 100$) cm. These bars were cut into six pieces to obtain six samples that were run on a CNC lathe in order to obtain high accuracy. Figure (1) represents the dimensions of the sample used for fatigue testing as per American Standard (ASTM) [21,22].

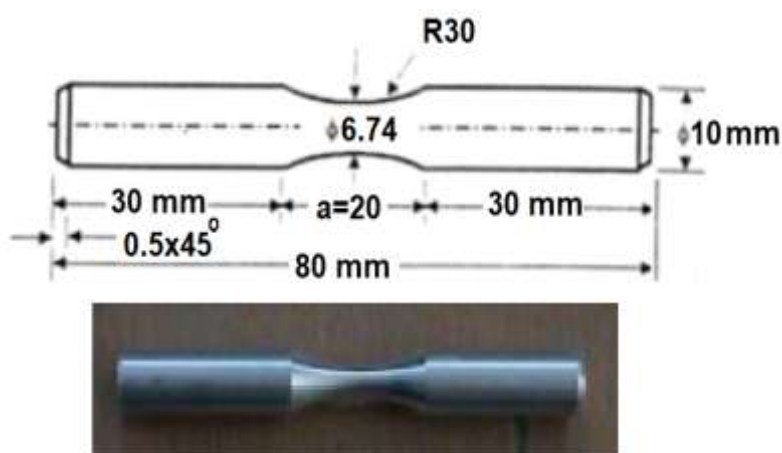


Figure (1): Fatigue Samples (ASTM) [21,22]

2.2 Chemical Composition

Table (1) shows the chemical analysis of the aluminum alloy 1050A used in the research. It was

conducted at the State Company for Inspection and Engineering Rehabilitation (SIER).

Table (1): The chemical composition of Pure Aluminum Alloys 1050A

1050A %	Si	Fe	Cu	Mn	Mg	Zn	Ti	Others	Al
Maximum	0.07	0.4	0.06	0.04	0.05	0.07	0.05	0.01	Balance

2.3 Mechanical properties of Aluminum Alloys 1050A

Three samples were examined on INSTRO (225) tensile tester by capacity 150 KN and the readout

rate was taken. Also checked the hardness on a Brinell Hardness Machine if I took six readings and extracted the average readings for the alloy as shown in table (2).

Table (2): The mechanical properties of Aluminum Alloys 1050A

Mechanical Properties	1050A
Ultimate tensile strength (MPa)	98
Yield stress (MPa)	50
Elongation%	7
Brinell hardness number (BHN)	27

2.4 The Fatigue Testing Machine

Avery Type 7305 rotary fatigue test was used at a speed of 1420 rpm in the center of the measurement and quality control device in order to test the samples, knowing that 3 samples were tested for each level of stress and extraction of the

rate in order to get rid of the scattering that occurs in the fatigue test, and this is the common context It is based on fatigue tests as shown as figure (2) and figure (3) show Fatigue Samples before & after Fatigue testing.



Figure (2): The Fatigue Testing Machine (Avery Type 7305). Figure (3): Fatigue Samples before & after testing

2.5 Track surface cracks

The replication technique was used to extract the lengths of the cracks where the crack length was calculated on the basis of the average length and from the following equation [19]:

$$a_{av} = \frac{a_{i+1} - a_i}{2} \quad \dots(2)$$

Then calculate the crack speed from the equation [13]

$$\frac{da}{dN} = \frac{\Delta a}{\Delta N} = \frac{a_{i+1} - a_i}{N_{i+1} - N_i} \quad \dots(3)$$

3. Results and experimental calculations

Three samples were exposed to different stresses, three samples were examined, and one crack was monitored in each sample. The results were as shown in Table (3).

Table (3): Samples and Stresses Loaded on it

Sample No.	Stress σ (MPa)	stress range $\Delta\sigma$ (MPa)	No. of failure cycles N_f (cycle)
1	80	160	1.5×10^5
2	95	190	5×10^4
3	110	220	2.8×10^4

3.1 The Fatigue Curve (S-N Curve) or Wohler Curve

The designer should know when to change the mechanical part subject to frequent and variable periodic stresses (dynamic loads), i.e. know the age of the part in advance in order to avoid sudden failure or sudden breakage, so the researchers tended to build a relationship between loads or repeated stresses (number of cycles) Failure of a piece or part, and this relationship is called the SN curve or Wohler curve and takes the following mathematical form.

$$\sigma_f = 723 N_f^{-0.185} \quad \dots\dots\dots(4)$$

From the above equation the fatigue limit = **36.6 MPa.**

3.2 Track Fatigue Cracks

The phases of the cracks are divided into three zones, as is evident from the experimental results in Table (4,5,6):

- a - From zero to the grain diameter, i.e. (20 μ m), it is (MSC), i.e. (Microstructurally Short Crack).
- b - From the grain diameter to one millimeter (PSC), meaning (Physically Short Crack).
- c - more than (1mm) is (LC), meaning (Long Crack).

Table (4): The practical results and their division into the three phases of the first fatigue sample

Sample No.= 1	Stress Range $\Delta\sigma = 160$ MPa	No. of Cycles to Failure $N_f = 150000$
Phase Crack	Crack Length a (μ m)	No. of Cycles N
MSC	10	133315
	14	136041

	18	141494
PSC	816	144220
	816	144220
LC	1020	145500
	1110	146200
	1190	146800
	1340	147200
	1372	147700
	Broken	150000

Table (5): The experimental results and their division into the three phases of the second fatigue sample

Sample No.= 2	Stress Range $\Delta\sigma = 190$ MPa	No. of Cycles to Failure $N_f = 50000$
Phase Crack	Crack Length a (μm)	No. of Cycles N
MSC	9	39113
	12	40258
	16	43693
PSC	244	45983
	850	48273
LC	1275	48960
	1666	49304
	2026	49532
	2222	49647
	2616	49761
	Broken	5000

Table (6): The experimental results and their division into the three phases of the third fatigue sample

Sample No.= 3	Stress Range $\Delta\sigma = 220$ MPa	No. of Cycles to Failure $N_f = 28000$
Phase Crack	Crack Length a (μm)	No. of Cycles N
MSC	8	16686
	12	21188
	18	22126
	340	23062

PSC	850	23814
	916	24562
LC	1232	25312
	1470	26438
	1786	27000
	2124	27336
	Broken	28000

As we mentioned earlier, these regions were divided in the practical results to make it easier to identify the above regions and to facilitate the extraction of constants in the models for each region, where MATLAB was used to design a program for organizing tables, extracting constants

and integrating equations, and to be a reference for researchers and postgraduate students because dictating the table with high accuracy is very stressful and takes a lot of time as shown as in tables (7,8,9).

Table (7): Practical calculations and their division into the three phases of the first fatigue sample

Sample No.		Stress Range ($\Delta\sigma$)		No. of Cycles to Failure (Nf)		
1		160 MPa		150000 cycle		
Crack Phase	Crack Length a (μm)	No. of Cycles N (cycle)	Crack Length Range Δa (μm)	No. of Cycles Range ΔN (cycle)	Crack Growth Rate $\Delta a/\Delta N(10^{-5})$ $\mu\text{m}/\text{cycle}$	Average Crack Length $a_{av}(\mu\text{m})$
MSC	10	133315	10	133315	7.501	5
	14	136041	4	2726	146.74	12
	18	141494	4	5453	73.354	16
PSC	816	144220	798	2726	29274	417
	816	144860	0	340	0	816
LC	1020	145500	204	940	21702	918
	1110	146200	90	700	12857	1065
	1190	146800	80	600	13333	1150
	1340	147200	150	400	37500	1265
	1372	147700	32	500	6400	1356
	Broken	150000	$\Sigma = 1372$	Failure	-	-

Table (8): Practical calculations and their division into the three phases of the second fatigue sample

Sample No.		Stress Range ($\Delta\sigma$)		No. of Cycles to Failure (Nf)		
2		190 MPa		50000 cycle		
Crack Phase	Crack Length	No. of Cycles	Crack Length Range	No. of Cycles Range	Crack Growth Rate	Average Crack Length
	a (μm)	N (cycle)	Δa (μm)	ΔN (cycle)	$\Delta a/\Delta N(10^{-5})$ $\mu\text{m}/\text{cycle}$	$a_{av}(\mu\text{m})$
MSC	9	39113	9	39113	23.01	4.5
	12	40258	3	1145	262.01	10.5
	16	43693	4	3435	116.45	14
PSC	244	45983	228	2290	9956.3	130
	850	48273	606	2290	26463	547
LC	1275	48960	425	687	61863	1062.5
	1666	49304	391	344	113666	1470.5
	2026	49532	360	228	157899	1846
	2222	49647	196	115	170433	2124
	2616	49761	394	114	345611	2419
	Broken	50000	$\Sigma=2616$	Failure	-	-

Table (9): Practical calculations and their division into the three phases of the third fatigue sample

Sample No.		Stress Range ($\Delta\sigma$)		No. of Cycles to Failure (Nf)		
3		220 MPa		28000 cycle		
Crack Phase	Crack Length	No. of Cycles	Crack Length Range	No. of Cycles Range	Crack Growth Rate	Average Crack Length
	a (μm)	N (cycle)	Δa (μm)	ΔN (cycle)	$\Delta a/\Delta N(10^{-5})$ $\mu\text{m}/\text{cycle}$	$a_{av}(\mu\text{m})$
MSC	8	16686	8	16686	47.944	4
	12	21188	4	4502	88.849	10
	18	22126	6	938	639.66	15
PSC	340	23062	322	936	34402	179
	850	23814	510	752	67819	595
	916	24562	66	748	8823.5	883
LC	1232	25312	316	750	42133	1074
	1470	26438	238	1126	21137	351
	1786	27000	316	562	56228	628
	2124	27336	338	336	100600	955
	Broken	28000	$\Sigma=2124$	Failure	-	-

4. Analyze and Discuss the Results

4.1 Analysis and discussion of microscopic short cracks (MSC)

The highest value that these cracks reach is as much as the diameter of the sample (20µm). Accordingly, the relationship was found between (D-a_{av.}) and the crack speed da/dN up to (20µm). Note Tables (7), (8) and (9) because when the value of (a) to (D), the cracking velocity is equal to zero, meaning that the cracking length reached the limits of the particle and thus stops, albeit for a very short period. Through the results of the crack lengths and the number of cycles shown in the above tables, a relationship was built assuming that the cracking speed is related to (D - a_{av.}) as follows [19] :

$$\frac{da}{dN} = A(D - a_{av.})^{\alpha_1} * \Delta\sigma^{\alpha_2} \dots\dots\dots(4)$$

To make it easier to solve this equation, it is reduced as follows:

$$\frac{da}{dN} = A_1(D - a_{av.})^{\alpha_1} \dots\dots\dots(5)$$

whereas:

$$A_1 = A\Delta\sigma^{\alpha_2} \dots\dots\dots(6)$$

Through the results in Tables (7), (8) and (9), a value can be found for each sample separately, and using the MATLAB program, the values of A1 and α₁ were found as shown in Table (10):

Table (10): the values of A1 and α₁

The first sample		The second sample		Third sample	
A ₁ *10 ⁻²	α ₁	A ₁ *10 ⁻²	α ₁	A ₁ *10 ⁻²	α ₁
1368	-1.6788	4586.6	-1.744	5904.8	-1.969

For simplicity, average values were taken and we found them to be equal to (-1.8). We prepared the same program to find out the relationship between

the stress range (Δσ) and the three (A1) values above, as shown in Table (11):

Table (11): the values of A1 and Δσ

The first sample		The second sample		Third sample	
A ₁ *10 ⁻²	Δσ (MPa)	A ₁ *10 ⁻²	Δσ (MPa)	A ₁ *10 ⁻²	Δσ (MPa)
1368	160	4586.6	190	5904.8	220

By using equation (6), the constants were found, and my agency is: A= 8.2534 * 10⁻¹⁰ & α₂ =

4.6619, and by substituting equation (6) in (5) is obtained:

$$\frac{da}{dN} = 8.2534*10^{-12} * \Delta\sigma^{4.6619} (D - a_{av.})^{-1.8} \dots\dots\dots(7)$$

Since this region is sandwiched between a slit length of zero and a particle diameter of 20 µm,

these values represent the limits of integration of equation (7), and thus the final equation

representing the fatigue life is obtained at this point:

$$N_{f1} = \frac{D^{2.8}}{2.8 * \Delta\sigma^{4.6619} * 8.2534 * 10^{-12}} = 1.91 * 10^{14} * \Delta\sigma^{-4.6619} \dots\dots\dots(8)$$

Where the units of $\Delta\sigma$ are MPa and N_{f1} represents the age of the sample in the first region in cycles. The above equation describes the behavior of cracks arising in the first grain, where it is clear that the main factors affecting the crack velocity da/dN are:

- a) The value of (D) or the particle size, where the higher the values of (D), the faster the cracking speed, and therefore it is preferable that the diameter of the particle be small to reduce the speed of cracking and thus increase the life of the sample or part, and this is consistent with what was stated in the source [13].
- b) The higher the stress, the greater the cracking speed. Therefore, it is preferable that the applied stresses be close to the fatigue limit of the material. In the case of making the stresses very high, the effect of the above equation is almost negligible because the small cracks end suddenly and have no effect, and this is

consistent with what was stated in the source [7].

4.2 Analysis and discussion of physical short cracks in the second region (PSC)

This region took the following mathematical formula [3]:

$$\frac{da}{dN} = A_2 * \Delta\sigma^{\alpha_3} * a \dots\dots\dots(9)$$

In the same previous method, in the first region, these constants were found, and they were as follows:

$$A_2 = 7.96 * 10^{15}, \alpha_3 = -8.17$$

Thus, we obtain the equation for the crack velocity or the rate of crack growth:

$$\frac{da}{dN} = 7.96 * 10^{15} * \Delta\sigma^{-8.17} * a \dots\dots\dots(10)$$

By integrating this equation from 20 μ m to 1000 μ m, the final equation for fatigue life in the second region is obtained:

$$N_{f2} = \frac{\ln(1000) - \ln(20)}{7.96 * 10^{15} * \Delta\sigma^{-8.17}} = \frac{\ln(1000)}{7.96 * 10^{15} * \Delta\sigma^{-8.17}} = \frac{2.306}{7.96 * 10^{15} * \Delta\sigma^{-8.17}}$$

$$N_{f2} = 2.9 * 10^{-16} * \Delta\sigma^{8.17} \dots\dots\dots(11)$$

Where the units of $\Delta\sigma$ are MPa and N_{f2} represents the age of the sample in the second region in cycles.

4.3 Analysis and discussion of the large cracks (LC) of the third region

From what has been mentioned above, these cracks have nothing to do with the granular size of the material, while the effect of cyclic stress is great. For simplicity, the same method was used in the previous areas to create an equation that

describes the movement of these cracks. This equation is known as (Paris equation), which is Equation (12) and as follows:

$$\frac{da}{dN} = C(\Delta K)^m \dots\dots\dots(12)$$

Where ΔK represents the range of the stress intensity coefficient, which is described by the following equation:

$$\Delta K = Y\Delta\sigma\sqrt{\pi a} \dots\dots\dots(13)$$

And by substituting equation (13) into equation (1) where Y represents (form factor) one-take delegation [5] and thus we get the following equation:

$$\frac{da}{dN} = C\Delta\sigma(\sqrt{\pi a})^m \dots\dots\dots(14)$$

The constants were extracted in the same way as before:

C = 3.34*10⁻⁶ & m = 3.1

The model that represents the crack velocity or the rate of crack growth in the area is as follows:

$$\frac{da}{dN} = 3.34*10^{-6} \Delta\sigma(\sqrt{\pi a})^{3.1} \text{ -----}(15)$$

By integrating this equation, since the limits of integration are from (1000 μm) to (6740 μm), which represents the diameter of the sample, we get the final equation in this region:

$$N_{f3} = \frac{82.91}{1.97*10^{-5} * \Delta\sigma} = 4.2*10^6 * \Delta\sigma^{-1} \dots\dots\dots(16)$$

Where the units of $\Delta\sigma$ are MPa and N_{f3} represents the age of the sample in the third region in cycles.

Equation (16) describes the movement of large cracks when the crack crosses the boundaries of the particle and leads to the failure of the

sample. In this research, we satisfied ourselves with five readings of the surface cracks for the following reasons:

1. The high difficulty in following the cracks under the microscope.
2. Follow-up and measurement of cracks takes a lot of time.
3. When the cracks become about 2-3 mm large, the process of merging the cracks begins.
4. It is possible to take more than three samples, as we followed the Hobson method [13] in order to reduce the time
5. It is clear from equation (16) that large cracks are not affected by the microscopic structure of the material, and when the applied stresses are high, they are effective.

Thus, the total fatigue life, which represents the age of the sample extracted from the proposed model in this research, is obtained for the three regions as follows

$$N_{ft} = N_{f1} + N_{f2} + N_{f3}$$

Whereas, N_{ft} is the number of total cycles (total) representing the age of the sample extracted from the proposed model in this research.

Many researchers, Hobson [3] and others, set the limit for the behavior of small cracks related to the grain size parameter, where the boundaries of the small cracks end when the crack reaches the end of the boundaries of the first grain, as shown in the figure (4).

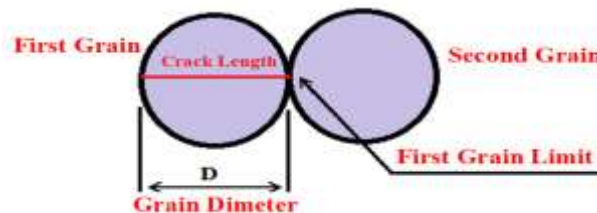


Figure (4): A schematic diagram of the boundaries of microscopic cracks

And they considered that what comes after that is a long fissure, that is, two stages of fissure growth, as in the schematic figure (5a).

But in this research, the lengths of the cracks were divided into three regions as follows: -

- i. From zero to the grain diameter, it is (MSC), that is (Microstructuly Short Cracks).
- ii. From the grain diameter to one millimeter (PSC), meaning (Physically Short Cracks).

- iii. more than (1mm) is (LC), meaning (Long Cracks).

This means that the short cracks stage is classified into two phases, after which it will be the third phase that represents the long cracks, as shown in Figure (5b).

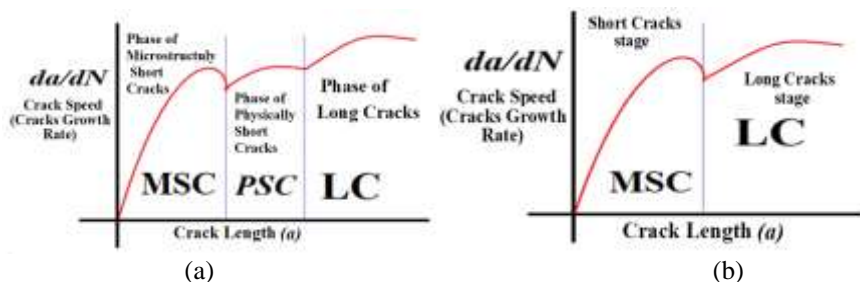


Figure (5): (a) relationship of crack speed to crack length, (b) Three stages of fatigue cracks growth in AA 1050A

In order to understand more accurately the importance of this region, the proposed model was

applied. Table (12) shows the results of the proposed three-stage model for crack growth:

Table (12): shows the results of the proposed three-stage model for crack growth:

Sample No.	Stress (MPa)	Experimental Nf	N _{f1}	N _{f2}	N _{f3}	N _{ft}
1	80	150000	10131	2951	26250	39332
2	95	50000	4547	1202	22106	27855
3	110	28000	3580	3981	19090	26650

By calculating the ages (Nf1 + Nf2 + Nf3), we note that the practical results that were extracted from the examination device when compared with the estimated results from the current model in Table No. (12) took the safe side, and thus it becomes clear that the current model gives a safer estimate, especially for the aluminum material from which it is made Aircraft tanks and pipeline

networks carrying fuel inside the aircraft, the subject of our research. The current model provides an appropriate safety factor ranging between (1.5-3.5), which encourages the designer to use it.

5. Conclusions

- 1- The growth of cracks in the aluminum alloy (1050A) used in the manufacture of fuel tanks for aircraft, as well as in the manufacture of pipe networks carrying fuel inside aircraft, was divided into three phases instead of two.
- 2- A mathematical model is proposed for the growth of cracks for each phase and the calculation of the age of each phase.
- 3- Short fatigue cracks grow under a range of stress intensity less than the threshold, and the concepts of linear elastic fracture mechanics cannot be applied in this case.
- 4- The growth rate of the fissure increases as the length of the fissure increases until it approaches the granular boundary, which represents the major obstacle to growth, at which point the growth rate decreases, and after passing this obstacle, growth begins to accelerate.
- 5- The growth of short fatigue cracks depends on the applied periodic stresses, crack length and particle size, while the growth of long fatigue cracks depends on the applied periodic stresses and crack length.
- 6- Estimating the ages of the samples subjected to periodic stresses. They were compared with other models and gave a more secure condition, which will lead to a higher stability for the aircraft tank designer when using the proposed model.
- 7- The total average length of the notch is equal to the final length of the notch.

References

- [1] N. Vikram and K. Raghuvir, "Review on Fatigue-Crack Growth and Finite Element Method." *International Journal of Scientific & Engineering Research* 4 (4): 833–43, **2013**.
- [2] L.C. Singal, S. G. Rajwinder and M. J. Aishna, "Fatigue Mechanical Life Design-A Review." *International Journal of Engineering Research and General Science* 5 (2): 247–51, **2017**.
- [3] Hobson, P., D., "The growth of short fatigue cracks in a medium carbon steel", thesis, university of Sheffield, U.K., **1985**.
- [4] A. B. Abdessalem, "Model selection, updating and prediction of fatigue crack propagation using nested sampling algorithm", 23^{ème} Congrès Français de Mécanique, Lille, 28 au 1er September **2017**.
- [5] R. I. Stephens, "Metal Fatigue in Engineering", Second Edition, Aweiley- Interscience Publication, John Wiley and sons, INC, **2011**.
- [6] A. Salmi & S. M. El-Amine, "Crack growth study under thermo-mechanical loads: parametric analysis for 2024 T3 aluminum alloy", Vol 13 No 50, October **2019**.
- [7] I. Mudasir, O. Faisal, E. Hassan, U. Mudaser, E. Marco, B.Saeed & G. Paolo, "Effect of Natural Aging and Fatigue Crack Propagation Rate on Welded and Non-Welded Aluminum Alloy (AA2219-T87)", *Advances in Science and Technology Research Journal (ASTRJ)*, Volume 13, Issue 3, September **2019**, pages 129–143.
- [8] Paris, P. & Erdogan, J. "A critical analysis of crack propagation laws", *Basic Eng. Trans. ASME*, 85, 528 (**1963**).
- [9] L. Hongjun, G. Jian and L. Qinchuan, "Fatigue of Friction StirWelded

- Aluminum Alloy Joints”, Appl. Sci. **2018**, 8, 2626; doi:10.3390/app8122626.
- [10] A. Haftirman, W. Haris , J. Andika, and N. A. Yahadi,” Effect of thickness on FCGof Aluminum alloys”, IOP Conf. Series: Materials Science and Engineering 343 (**2018**).
- [11] Alalkawi H. J. M, Ali Yousuf Khenyab, Abduljabar H. Ali “Improvement of Mechanical and Fatigue Properties for Aluminum Alloy 7049 By Using Nano Composites Technique”, **Al-Khwarizmi Engineering Journal**, Vol. 15, No. 1, March, (2019), P.P. 1- 9.
- [12] Abdullah Dhayea Assi & Rawa Hamed M. ALKalali ,”Fatigue Limit Prediction Based on Hardness for Both Steel and Aluminum Alloys”, IOP: Materials Science and Engineering, Vol. 1105, No.012044, 2021, Pp. 1-11
- [13] M N Abdulridah, Abdullah Dhayea Assi and H J Al-Alkawi, “Influence of Cryogenic Temperature (CT) on Tensile Properties and Fatigue Behavior of 2024-Al₂O₃ Nanocomposites”, ICEMEA-2020, IOP Conf. Series: Materials Science and Engineering 765 (**2020**) 012052.
- [14] Shaima A. Hamza, “The effect of constant and variable amplitude loads on the fatigue life of an alloy of low carbon steel.” Babel Journal / Pure and Applied Sciences and Engineering Sciences, Volume 26, Issue 1: **2018**.
- [15] Abdullah Dhayea Assi & Salman Hussien Omran, “The Effect of Welding Joints Design on the Fatigue Crack Growth Rate”, IEEE Xplore, 2020 6th International Engine, 26-27 Feb. 2020, Erbil, Iraq,
- [16] Rusul Kh. Abd & Nawal J. Hammad , “Estimating Pitting Corrosion Depth and Density on Carbon Steel (C-4130) using Artificial Neural Networks”, **Journal of Engineering**, Number 5 Volume 28 May **2022**, <http://www.joe.uobaghdad.edu.iq/>
- [17] Abdullah D.A. & Salman H. O.,” The effect of tempering on the fatigue Behavior for medium carbon steel”, the Iraqi Journal For Mechanical and Material Engineering, Vol.11, No.4, **2011**.
- [18] Haider Hadi Jasim, “Evaluation of Fatigue Behavior of Epoxy Based Coatings used for Potable Water Storage Tanks”, **Journal of Engineering**, No. 3 Vol. 26 January **2020**, <http://www.jcoeng.edu.iq>.
- [19] Abdullah Dhayea Assi “study of Fatigue crack growth in (**2219**) Aluminum Alloy under Cyclic Stresses”, Journal of Techniques, Vol. 2, No.4, **2020**, Pp.33-46.
- [20] S.L. Sabater, Fundiciones ,SABATER FUNDIMOL,Catalogo,2004-2014.
- [21] ASTM E647-05, 2005, “Standard Test Method for Measurement of Fatigue Crack Growth Rates,” Annual Book of ASTM Standards, Vol. 03.01, ASTM International, West Conshohocken, PA, pp. 1–41.
- [22] MatWeb.com, Material Property Data, 2019.

Appendix-A

```

TAPLE.m x +
1 -   clc,clear,close all
2 -   SNo = input('inpu The No. of Specimen :n = ');
3 -   a = input('inpu The Crack Length of a = ');
4 -   N = input('inpu The The No. of Cycles= ');
5 -   n=length(a);sda=0;
6 -   for i=1:n
7 -       if i <=10
8 -           da(i)=a(i+1)-a(i); sda=sda+da(i); dN(i)=N(i+1)-N(i);
9 -           aav(i)=(a(i+1)+a(i))/2;
10 -        end
11 -    end
12 -    sumda=sda,a_final=a(n),digits(5);daN=da./dN;daN=vpa(daN);daN=daN*100000;
13 -    disp('-----')
14 -    disp('          Experimental Procedure and Results of Crack Growth ')
15 -    disp('-----')
16 -    disp([' The Specimen No. = ',num2str(SNo)])
17 -    disp([' a =',num2str(a),'])
18 -    disp([' N =',num2str(N),'])
19 -    disp('-----')
20 -    disp('          Results Taple')
21 -    disp('-----')
22 -    disp('   da           dN           da/dN*10^-5           aav')
23 -    disp('-----')
24 -    for i=1:n
25 -        disp(sprintf('%4d %16.5g %16.5g %16d', da(i),dN(i), daN(i),aav(i)))
26 -        disp('-----')
27 -    end
    
```

Figure (6) the MATLAB program to organize the crack tracking table

Experimental Procedure and Results of Crack Growth for Specimen No.= 1											
a =	[0	10	14	18	816	816	1020	1110	1190	1340	1372]
N =	[0	133315	136041	141494	144220	144560	145500	146200	146800	147200	147700]
Results Taple											
da	dN	da/dN*10^-5	aav								
10	1.3332e+05	7.501	5								
4	2726	146.74	12								
4	5453	73.354	16								
798	2726	29274	417								
0	340	0	816								
204	940	21702	918								
90	700	12857	1065								
80	600	13333	1150								
150	400	37500	1265								
32	500	6400	1356								

Figure (7) Application of the program on the practical results of the first fatigue sample from Table (4)

Experimental Procedure and Results of Crack Growth for Specimen No.= 2										
a = [0 9 12 16 244 850 1275 1666 2026 2222 2616]										
N = [0 39113 40258 43693 45983 48273 48960 49304 49532 49647 49761]										
Results Table										
da	dN	da/dN*10 ⁻⁵		aav						
9	39113	23.01		4.500000e+00						
3	1145	262.01		1.050000e+01						
4	3435	116.45		14						
228	2290	9956.3		130						
606	2290	26463		547						
425	687	61863		1.062500e+03						
391	344	1.1367e+05		1.470500e+03						
360	228	1.579e+05		1846						
196	115	1.7043e+05		2124						
394	114	3.4561e+05		2419						

Figure (8) Application of the program on the practical results of the second fatigue sample from Table (5)

Experimental Procedure and Results of Crack Growth for Specimen No.= 3											
a = [0 8 12 18 340 850 916 1232 1470 1786 2124]											
N = [0 16686 21188 22126 23062 23814 24562 25312 26438 27000 27336]											
Results Table											
da	dN	da/dN*10 ⁻⁵		aav							
8	16686	47.944		4							
4	4502	88.849		10							
6	938	639.66		15							
322	936	34402		179							
510	752	67819		595							
66	748	8823.5		883							
316	750	42133		1074							
238	1126	21137		1351							
316	562	56228		1628							
338	336	1.006e+05		1955							

Figure (9) Application of the program on the practical results of the third fatigue sample from Table (6)